The First Ground-Level Enhancement of Solar Cycle 24 on 17 May 2012 and Its Real-Time Detection

**A. Papaioannou · G. Souvatzoglou · P. Paschalis ·
M. Gerontidou · H. Mavromichalaki**

Abstract Ground-level enhancements (GLEs) are defined as sudden increases in the recorded intensity of cosmic-ray particles, usually by neutron monitors (NMs). In this work we present a time-shifting analysis (TSA) for the first arriving particles that were detected at Earth by NMs. We also present an automated real-time GLE alert that has been developed and is operating via the Neutron Monitor Database (NMDB), which successfully identified the 17 May 2012 event, designated as GLE71. We discuss the time evolution of the real-time GLE alert that was issued for GLE71 and present the event onset-time for NMs that contributed to this GLE alert based on their archived data. A comparison with their real-time time-stamp was made to illustrate the necessity for high-resolution data (*e.g.* 1-min time resolution) made available at every minute. The first results on the propagation of relativistic protons that have been recorded by NMs, as inferred by the TSA, imply that they are most probably accelerated by the coronal-mass-ejection-driven shock. Furthermore, the successful usage of NM data and the corresponding achievement of issuing a timely GLE alert are discussed.

A. Papaioannou (✉) · G. Souvatzoglou · P. Paschalis · M. Gerontidou · H. Mavromichalaki
Nuclear and Particle Physics Section, Physics Department, National and Kapodistrian University of Athens, Athens, Greece
e-mail: atpapaio@phys.uoa.gr

H. Mavromichalaki
e-mail: emavromi@phys.uoa.gr

A. Papaioannou
Institute for Astronomy, Astrophysics, Space Applications and Remote Sensing, National Observatory of Athens, Athens, Greece
e-mail: atpapaio@astro.noa.gr

G. Souvatzoglou
ISNET Co, Athens, Greece
e-mail: gsouv@isnet.gr

1. Introduction

Ground-level enhancements (GLEs) comprise the high-energy end of solar energetic parti-
cles and constitute a special class of events in which ions are accelerated to relativistic ener-
gies, causing a significant sudden increase of cosmic rays at ground-based detectors, mainly
at neutron monitors (NMs) (Forbush, 1946). To date, 71 such events have been identified
since the initiation of reliable recordings, which began in the 1950s (Miroshnichenko and
Perez-Peraza, 2008; Gopalswamy, Xie, and Usoskin, 2010). The mean occurrence rate of
GLEs is almost one per year, with a slight deviation due to intense solar activity around solar
maximum (Andriopoulou *et al.*, 2011; Papaioannou *et al.*, 2011). The most recent event was
recorded on 17 May 2012, designated as GLE71 (Mavromichalaki and Souvatzoglou, 2012;
Kudela, 2013).

These solar cosmic-ray events are associated with both fast coronal mass ejections
(CMEs) and intense solar flares (Gopalswamy, Xie, and Usoskin, 2010; Gopalswamy *et al.*,
2012; Nitta *et al.*, 2012). Although solar flares were thought to be the sole source for
the occurrence of GLEs, the importance of CMEs was also recognized later on (Kahler,
Hildner, and Van Hollebeke, 1978). The study of GLEs and the role of CMEs and so-
lar flares in the production of very energetic particles are often controversial. This is
based on the argument that there are two particle acceleration mechanisms, the flare re-
connection and the shock evolution (Bazilevskaya, 2009; Reames, 2009; Kudela, 2009;
Vainio *et al.*, 2009), and both processes are expected to operate during major eruptions
such as those involved in GLEs (Gopalswamy *et al.*, 2012; Firoz *et al.*, 2012).

A variety of direct and indirect effects on geo-space, humans, industry, and econ-
omy are caused by GLEs. These effects include risks and failures at communication and
navigation systems, spacecraft electronics and operations, space power systems, manned
space missions, and commercial aircraft operations. The main effect of GLEs is the en-
hancement of radiation exposure. On commercial aircraft operations the loss of high-
frequency communication and, at extreme polar latitudes, an increase in the radiation
exposure above that experienced from the background Galactic cosmic radiation is ex-
pected (Shea and Smart, 2012). Therefore, it is crucial to establish a real-time opera-
tional system that would be in place to issue reliable and timely GLE alerts. To this
end, data from the worldwide network of NMs could be used (Dorman *et al.*, 2004;
Mavromichalaki *et al.*, 2004).

In response to this necessity, the Neutron Monitor Database (NMDB) (http://www.nmdb.
eu), a project funded by the Seventh Framework Programme of the European Commission
aimed at creating a real-time database with high-resolution cosmic-ray data (Steigies, 2008a,
2008b; Mavromichalaki *et al.* 2010a, 2011). A digital repository for cosmic-ray data has
been set up, whose central database contains NM data acquired in the past 50 years together
with new continuously updated observations from 47 NMs with 1-min and 1-h resolution,
operated by the institutes that constitute the NMDB consortium as well as external partners
(Mavromichalaki *et al.*, 2011).

In this work we demonstrate some first results on the propagation of the relativistic pro-
tons that were registered by NMs during GLE71. Furthermore, we present the automated
real-time GLE alert that has been developed by the Athens cosmic ray group. This operates
via NMDB and successfully identified the recent GLE71. The time evolution of the real-
time GLE alert that was issued for this event and the calculation of the event onset-time for
different NMs that contributed to this GLE alert based on their archived data are discussed to
illustrate the necessity for high-resolution data (hereafter 1-min time-resolution data) made
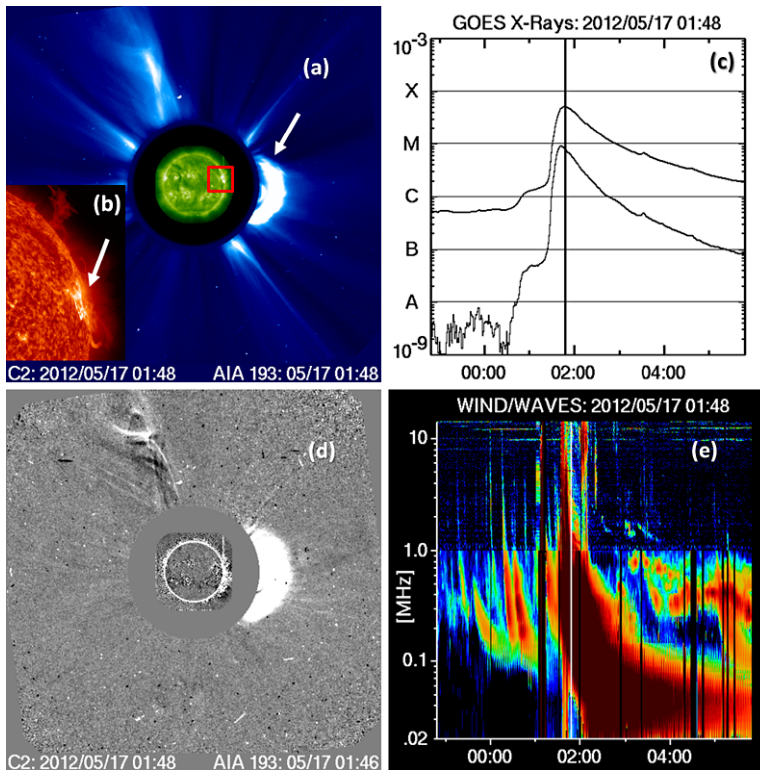available at every minute.

Figure 1 CME (a, d), M5.1 soft X-ray flare (c), and radio bursts (e) associated with the 17 May 2012 GLE event. The CME can be seen in the SOHO/LASCO difference images at 01:48 UT with EIT difference images showing the disk activity. The CME is marked with an arrow in (a). The embedded figure from SDO AIA 304 in (a), indicated as (b), shows the solar flare, and an arrow marks its position. The approximate flare location is indicated by a red square in (a). The vertical lines in the GOES plot (c) and the *Wind*/WAVES dynamic spectrum (e) mark the time of the corresponding LASCO frames on the left.

2. Background of the 17 May 2012 Event

2.1. Solar Activity

On 17 May 2012, the main sunspot group was active region AR11476. It produced a strong M5.1 solar flare, which started at 01:25 UT and peaked at 01:47 UT (Figure 1(c)). At that time this active region was situated at N13W83 on the Sun (Figure 1(b)). The flare was accompanied by a halo CME, which was successfully recorded by the *Solar and Heliospheric Observatory* (SOHO)/*Large Angle and Spectrometric Coronagraph*(LASCO) (Figures 1(a) and 1(d)) as well as by the *Solar TErrestrial RElations Observatory* (STEREO) A and B coronagraphs (Kaiser *et al.*, 2008) (Figure 2). SOHO/LASCO pinpointed the beginning of the CME at 01:48 UT. Its linear speed was evaluated to be 1582 km s^{-1}. Both STEREO spacecraft observed the initiation of the CME at 01:45 UT, while the CACtus online CME catalog (Robbrecht and Berghmans, 2004) provides a start time of 02:12 UT and a linear speed of 1302 km s^{-1}. Type III and type II radio bursts were recorded by *Wind*/WAVES (Figure 1(e)). A closer look at the available solar data reveals more details. The type III radio burst that signified the release of relativistic electrons into open magnetic field lines
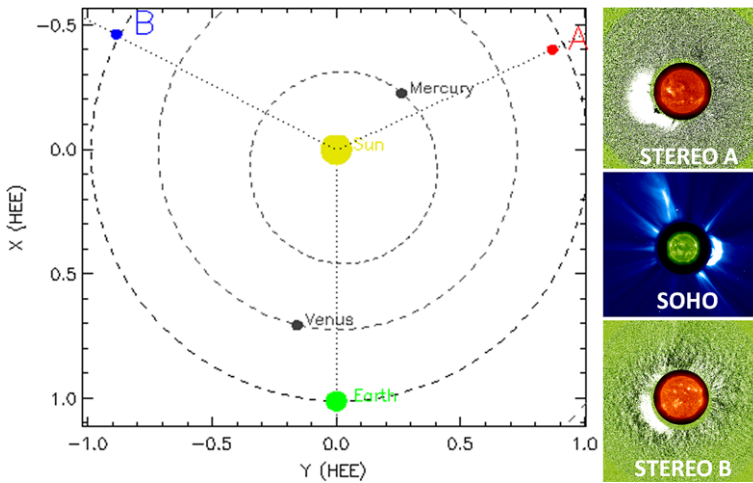
Figure 2 The halo CME of 17 May 2012 as it was recorded by STEREO-B (right bottom panel), SOHO/LASCO (right middle panel), and STEREO-A (right upper panel). The left part shows the position of the STEREO spacecraft with respect to the Earth on 17 May 2012 at 01:50 UT. The separation angle between STEREO A and B was 127.551° (The left part of this figure was created at http://stereo-ssc.nascom.nasa.gov/where.shtml).

was spotted by STEREO A and B and also from *Wind* at L1 (Figure 3). The electromagnetic emissions started at around 01:33 UT and ended at 01:44 UT. The type II burst, indicating a shock, was recorded by STEREO A and *Wind* at 01:40 UT, but was not seen by STEREO B. The *Reuven Ramaty High Energy Solar Spectroscopic Imager* (RHESSI; Lin *et al.*, 2002) observed the solar flare that started at 01:38 UT and peaked at 01:40 UT.[1] Signatures of this event were clearly seen in hard X-ray (HXR) and γ-ray emissions up to 20 MeV. Therefore, once again, the processes of the flare reconnection and the shock formation could have taken place during these major eruptions, resulting in GLE71.
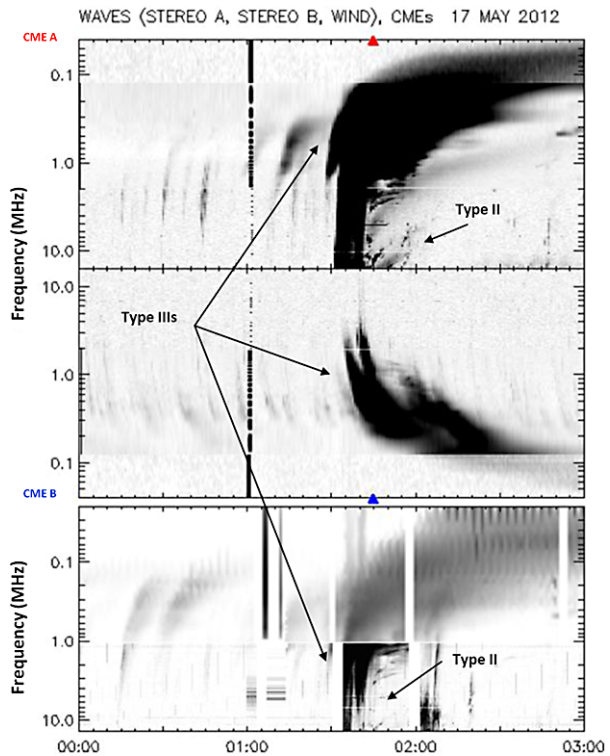
2.2. Neutron Monitor Recordings

Different NMs present different time profiles for a given GLE because of different asymptotic look angles and rigidities corresponding to the anisotropic nature of the particle streams (Bieber *et al.*, 2002; Moraal and McCracken, 2012; Nitta *et al.*, 2012). Differences among the time profiles of the cosmic-ray intensity as it was recorded by the Oulu (OULU), Apatity (APTY), Fort Smith (FSMT), and South Pole (SOPO) NMs during the GLE71 are clearly visible in Figure 4. The first relativistic protons that arrive at Earth propagate along the interplanetary magnetic field (IMF). Therefore, a NM whose asymptotic look angle is nearly aligned with the IMF is characterized by a low vertical cut-off rigidity (< 1 GV) and is expected to give the earliest onset and highest increase in count rate (Bombardieri *et al.*, 2007; Nitta *et al.*, 2012). It is important to note that these are the NMs that are essential for the timely operation of the real-time GLE alert software. For this reason we used these NMs in our analysis.

An algorithm that determines the onset time at a given NM count rate, as well as the time of the maximum increase and the maximum variation, has been developed by the

---

[1]http://hesperia.gsfc.nasa.gov/hessidata/dbase/hessi_flare_list.txt.

Figure 3 Radio spectrograms recorded by the SWAVES instruments onboard STEREO A (top panel), STEREO B (middle panel), and *Wind*/WAVES (bottom panel) provided by the Meudon Radio Monitoring Survey (http://secchirh.obspm.fr/select.php). The blue and red arrows denote the arrival time of the CME at STEREO B and A, respectively

Athens cosmic-ray group and has been applied to the measurements of the NMs used in this study, APTY, OULU, FSMT, and SOPO. The algorithm compares the count rate of a specific pre-event period set by the user with the data immediately preceding it. In that sense, the user defines a background time-period for which the algorithm calculates the average counting rate $\langle I \rangle$ and the standard deviation σ inside the specified time window. Then the algorithm compares the data with a threshold $\langle I \rangle + n\sigma$, where n can be selected by the user. When a number of m consecutive measurements fulfill this condition, the onset is defined as the time-stamp of the first measurement that exceeds the threshold. Furthermore, the algorithm reads the data and marks the highest value of the count rate as well as its time-stamp. We used 2-min averaged data for all NMs. The background time-period used to normalize the data was set to be from $00:00-01:00$ UT on 17 May 2012. The threshold was defined as $\langle I \rangle + 3\sigma$ and the consecutive points exceeding the threshold were set to $m = 4$.

As can be deduced from Figure 4, during GLE71 the flux remained above the background level for almost one and a half hours. The NMs situated at South Pole (SOPO and SOPB; the latter not shown) recorded the most intense fluxes during GLE71. Apatity NM (APTY) was the first NM that recorded the arrival of relativistic protons at Earth (Table 1). The rapid rise as shown by the APTY NM intensity time-profile (Figure 4) indicates that relativistic protons had reasonable access to the Sun-Earth-connecting field lines. Inspection of the NM data from various stations around the world showed that the event was recorded by NMs with a vertical cut-off rigidity up to ≈ 2 GV, indicating that there were particles with this vertical cut-off rigidity. The Moscow NM, with a vertical cut-off rigidity of 2.43 GV, recorded an increase of marginal significance that may or may not be related to GLE71.
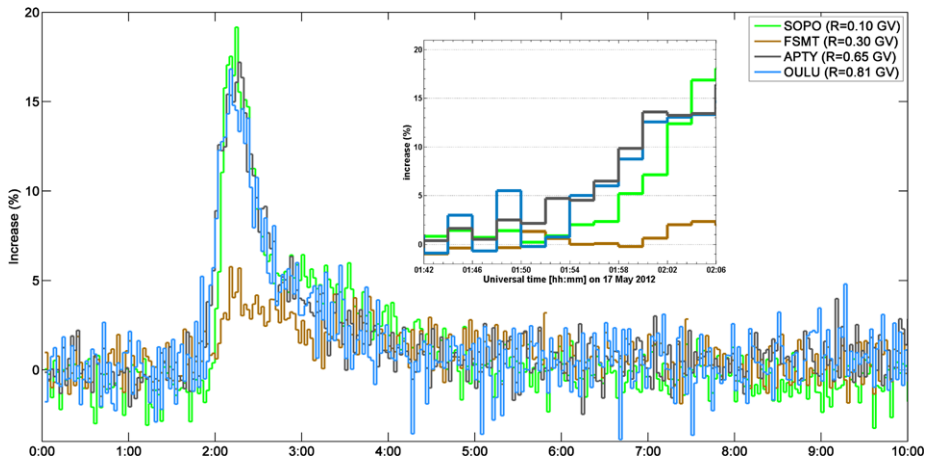
Figure 4 The ground-level enhancement of 17.05.2012 (GLE71) as it was recorded by the OULU (blue), APTY (gray), FSMT (brown), and SOPO (green) NMs. A zoom of the rising phase of GLE71 as this was recorded by the NMs (the same color code has been applied) from 01:42 to 02:06 UT; it is presented in the inset.
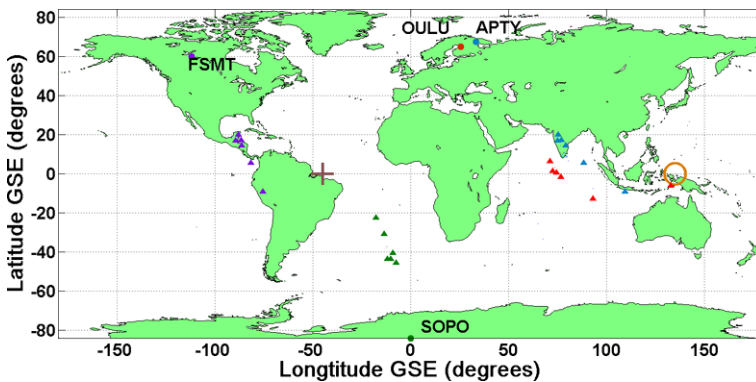

Figure 5 Viewing directions of neutron monitors in the GSE coordinates at 01:50 UT on 17 May 2012. Geomagnetic conditions were slightly disturbed (Kp = 2; Dst = −34 nT). The plus (+) and empty-circle (○) signs designate the position of the nominal anti-sunward and sunward field directions, respectively. Stations displayed are Apatity (APTY) in blue, Oulu (OULU) in red, Fort Smith (FSMT) in purple, and South Pole (SOPO) in green. The asymptotic directions are presented as triangles, the stations as circles. The same color has been used for the station and its asymptotic cones.

Crucial parameters, such as the onset and maximum times and the maximum increase for the OULU, APTY, FSMT, and SOPO NMs are presented in Table 1. Column 1 provides the name of the NM used in the analysis, column 2 the vertical cut-off rigidity (in GV) of the NM station, columns 3 and 4 the longitude and latitude of the station (in °), column 5 the onset time (in UT), column 6 the maximum time (also in UT), and column 7 the maximum increase (in %) of the NM station. All products were calculated based on 2-min NM data.

Table 1 Characteristics of GLE71 as recorded by the SOPO, FSMT, APTY, and OULU NMs

Neutron monitor	Vertical cut-off rigidity (GV)	Longitude (°)	Latitude (°)	Onset time (UT)	Maximum time (UT)	Maximum increase (%)
SOPO	0.10	N/A	90 S	01:58	02:12	19.17
FSMT	0.30	111.93 W	60.02 N	02:00	02:08	5.77
APTY	0.65	33.4 E	67.57 N	01:50	02:14	17.19
OULU	0.81	25.47 E	65.05 N	01:54	02:08	16.18

Figure 5 shows the viewing directions (Shea, Smart, and Flückiger, 2000; Vashenyuk, Balabin, and Gvozdevsky, 2009) of the NMs used in this analysis at around the onset of GLE71 (01:50 UT) for particles of 1 to 2.5 GV. The APTY and OULU NMs have similar viewing directions, which are very close to the nominal sunward direction (as is indicated by the empty-circle sign in Figure 5). The SOPO and FSMT NMs present viewing directions close to the nominal anti-sunward direction (indicated by the plus sign in Figure 5). The APTY and OULU NMs observed an earlier onset and exhibited a more rapid rise than the SOPO and FSMT NMs. The SOPO NM (together with SOPB – not shown), although shifted slightly further from the nominal sunward direction, recorded the most intense flux during GLE71 (see Table 1 and Figure 4). This is expected because the location of the station(s) is ideal for GLE tracking. The SOPO NM is a high-latitude station with a vertical cut-off rigidity of 0.10 GV (see Table 1). It is also located at a high altitude (≈ 2820 m), which provides the advantage of detecting a small event with a clear profile. In a real sense, it is closer to outer space than any other monitor on Earth. (Kuwabara *et al.*, 2006; Belov *et al.*, 2010). The FSMT NM, whose viewing directions are closer to the nominal anti-sunward direction (see Figure 5), exhibits a slower rise and a mild maximum increase (5.77 %, see Table 1).

2.3. Time-Shifting Analysis

For the first arriving particles it is possible to perform time-shifting analyses (TSA; Malandraki *et al.*, 2012; Vainio *et al.*, 2013). The NMs recorded particles of very high energy (≥ 500 MeV). According to Clem and Dorman (2000), a low-end energy limit of particles recorded by a NM station is ≈ 1 GV (*i.e.* 433 MeV). The corresponding mean velocity for such relativistic protons would be $u = 0.73c$. The length of the Parker spiral L can be computed based on the solar wind speed during the event as follows (Vainio *et al.*, 2013): we assume that the spiral length L that is traveled by the particles is the spiral from the center of the Sun to 1 AU minus the spiral from the center of the Sun to its edge (*i.e.* the distance equal to 1 solar radius R_s) according to

$$L = z(1 \text{ AU}) - z(R_s), \tag{1}$$

where

$$z(r) = \frac{a}{2}\left[\ln\left(\frac{r}{a} + \sqrt{(1 + r^2/a^2)} + \frac{r}{a}\sqrt{(1 + r^2/a^2)}\right)\right], \tag{2}$$

and $a = u_{sw}/\Omega$ given that Ω corresponds to the sidereal rotation period (*i.e.* $2\pi/\Omega =$ 24.47d). During GLE71, the solar wind speed u_{sw} measured by the *Advanced Composition Explorer* (ACE)/*Solar Wind Electron, Proton, and Alpha Monitor* (SWEPAM) (McComas

et al., 1998) was slow ≈ 380 km s^{-1}, leading to $L = 1.15$ AU. For the first arriving particles we assumed scatter-free propagation and calculated the expected release time of the relativistic protons, t_{release}, adding 8.33 min for comparison with ground-based measurements (*e.g.* radio burst),

$$t_{\text{release}} = t_{\text{onset}} - \frac{L}{u} + 8.33 \text{ (UT)}. \tag{3}$$

We applied this formulation to the recordings of the APTY NM station and obtained $t_{\text{onset}} = 1:50$ UT (see Table 1). The travel time of the relativistic protons of ≈ 1 GV was calculated to be ≈ 13 min and the corresponding anticipated release time is $\approx 01:45$ UT.

2.3.1. Relation to Solar Sources

The TSA that was performed in Section 2.3 provides an estimate of the latest possible release time of relativistic protons from the Sun that is consistent with the determined onset time at Earth at APTY NM. Because there are hard X-rays and γ-rays from the RHESSI data one might conclude that the protons responsible for the GLE have been released at the flare (Watanabe *et al.*, 2006; Grechnev *et al.*, 2008). A comparison of the release time of the first arriving particles with the time of an efficient generation of protons in the flare provides a first hint for the solar source of these particles. A recent study by Kurt *et al.* (2013) has shown that if the first arriving particles are delayed with respect to HXR and γ-ray emissions by $3 - 5$ min, these protons are accelerated at the flare. Given the time lag between the HXR emissions and the GLE particle-release time, the first arriving particles recorded at the APTY NM station would probably be attributed to the shock that was marked as the type II burst at 01:40 UT, which was formed at $\approx 4 R_s$ at 01:48 UT. This takes into account that the acceleration timescale for the simple first-order Fermi (shock) acceleration for the 433 MeV particles would be ≈ 7 min, according to the formula $\approx 0.16\beta P$(GV) h, where β is the particle velocity in terms of light speed ($\beta = uc^{-1}$) and P is the rigidity (Caballero-Lopez, Moraal, and McDonald, 2004; McCracken, Moraal, and Shea, 2012). It is also noteworthy that the flare size (M5.1) associated with GLE71 was rather small for such an event (*i.e.* GLE), while the speed of the CME was very high (1582 km s^{-1}), which is typical for GLEs (Gopalswamy *et al.*, 2012). Therefore GLE71 was most probably linked to the CME driven-shock and not to the flare. Nevertheless, it should be noted that TSA is a rough approximation and provides a first insight only into the propagation of the particles within the limitations of the assumptions.

3. The GLE-Alert Algorithm and Its Real-Time Performance

3.1. The Work Scheme of the GLE-Alert Algorithm

The NMs record particles of highest energies (≥ 500 MeV). Consequently, extreme solar-energetic-particle (SEP) events are being recorded by NMs very promptly, within several minutes (Gopalswamy *et al.*, 2012). This is the foundation of the physical concept of the GLE-alert software. The early detection of Earth-directed solar cosmic-ray particles by NMs results in preventive SEP monitoring, leading to an alert with a very low false-alarm probability (Dorman and Zuckerman, 2003; Dorman *et al.*, 2004; Kuwabara *et al.*, 2006). To this end, the worldwide distribution of NMs at several locations with unique characteristics such

as altitude, latitude, and geomagnetic cut-off and their integration into networks has proven to be an essential asset (Mavromichalaki, 2010). A GLE-alert code was implemented by the cosmic-ray group of the National and Kapodistrian University of Athens (Souvatzoglou *et al.*, 2009) and was set into operation in real-time mode within NMDB (Mavromichalaki *et al.*, 2010b).

The work scheme of the GLE-alert algorithm has been thoroughly presented in a series of published works (*e.g.* Souvatzoglou *et al.*, 2009; Mavromichalaki *et al.*, 2010b; Papaioannou *et al.*, 2011), and we do not focus on it here. Nevertheless, for reasons of completeness, a summary of this scheme and the crucial points of the GLE alert unfolding are summarized here. For each NM station a moving threshold is being defined as $I_{th} = M + N\sigma$, where σ is the standard deviation, M the average of the previous 60-min measurements, and N is a statistical factor that characterizes each station. The value of N varies from 1 to 3 (Souvatzoglou *et al.*, 2009). When a new recorded value exceeds the threshold, a pre-alert point is marked. If three pre-alert points are marked in succession, a *station alert* signal is produced. This is the so-called *warning* stage of the GLE alert. A supervising program, with a time window of 15 min, is enabled immediately after the first NM enters the *station alert* mode. If three NMs independently of each other enter the *station alert* mode within that specific time window, a *general alert* is produced (Mavromichalaki *et al.*, 2010b).

Possible users of the GLE alert may retrieve all related information on the general GLE alert via the NMDB web portal (http://www.nmdb.eu/?q=node/19), under data products. This information includes the *station-alert* evolution in numerical form for each NM that participates in NMDB and in the GLE-alert software, the NMs that contribute to establishing the *general alert*, and current conditions (*quiet, watch, warning, alert*). There is also a graphical interface available that displays the evolution of the *station alert* for each NM station and the overall *general alert* in color bars (Mavromichalaki *et al.*, 2010b).

3.2. Performance of the Real-Time GLE-Alert Software

The first GLE of solar cycle 24 (GLE71) was detected by the GLE-alert algorithm operated via NMDB in real-time at 02:13 UT. The first NM station entering the *station-alert* mode was APTY. According to its real-time performance, APTY entered the *station-alert* mode at 01:59 UT while the first pre-alert point (see Section 3.1) was marked at 01:55 UT (see Table 2). This agrees with Table 1, because the APTY station was the first that recorded an abrupt enhancement in its count rate. The OULU NM, and consequently the FSMT NM, entered the *station-alert* mode at 02:10 UT and 02:13 UT, respectively, leading to a *general alert* at 02:13 UT (see Table 2 and Figure 6). Column 1 in Table 2 denotes the GLE-alert server clock (in UT), column 2 shows the relevant *station-alert* level of the specific NM station as deduced by its moving threshold (see Section 3.1 and Mavromichalaki *et al.*, 2010b for details), columns 3 and 4 provide the time-stamp (in UT) and the measured counts sent by the NM station to NMDB in real-time. These latter three columns are repeated in sequence for every NM acting as a seeder of the GLE-alert algorithm, which in this case are APTY, FSMT, OULU, and SOPO.

Figure 6 and Table 2 highlight useful details of the real-time evolution of the GLE alert. The APTY NM station provides its data to the NMDB server, with a time lag of almost 1 min compared to the GLE-alert server clock (see columns 2 and 4 of Table 2). That means that the data flow from APTY NM is close to continuous and the time synchronization with respect to the GLE-alert server clock lagged behind by only about 1 min (see Table 2), leading to a very reasonable behavior of this NM station upon application of the GLE-alert software in real-time. Other NMs used in this study provided their data with larger time-lags. This implies that both the data flow of the NM stations and their time synchronization

Table 2 The evolution of the real-time GLE alert for GLE71 based on the SOPO, APTY, FSMT, and OULU NMs, as well as the timing of the *station alert*. The *general alert* occurs when the third NM in succession enters the *station-alert* mode, *i.e.* at 02:13 UT. The 'server time' and 'time stamp' are in UT, the 'alert level' indicates how many consecutive times the NM station exceeds its threshold, and 'value' refers to the count of the NM send at that specific time-stamp to NMDB.

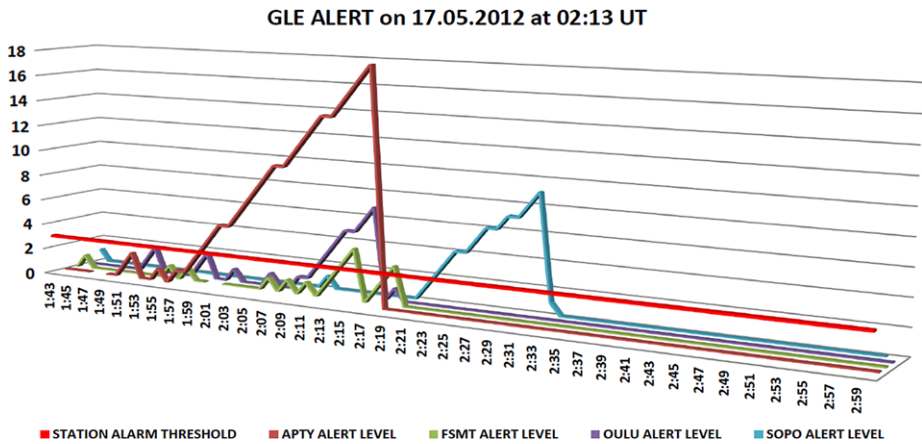| GLE-alert server	APTY			FSMT			OULU			SOPO			Station alert
Server time	Alert level	Time-stamp	Value	Alert level	Time-stamp	Value	Alert level	Time-stamp	Value	Alert level	Time-stamp	Value	
2012.05.17 1:56:19	1	1:55	11008	1	1:53	13363	1	1:54	6794	0	1:39	20592	
2012.05.17 1:57:35	1	1:55	11008	0	1:54	13044	2	1:56	6858	0	1:39	20592	
2012.05.17 1:58:20	2	1:56	10948	0	1:56	13029	2	1:56	6858	0	1:39	20592	
2012.05.17 1:59:20	3	1:58	11209	0	1:56	13029	0	1:57	6650	0	1:42	20998	APTY (1:59)
2012.05.17 2:00:21	4	1:59	11521	0	1:57	13014	1	1:58	7016	0	1:42	20998	
2012.05.17 2:01:21	5	2:00	11586	0	1:58	13008	1	1:58	7016	0	1:43	20176	
2012.05.17 2:02:36	5	2:00	11586	0	1:59	12955	0	1:58	7016	0	1:43	20176	
2012.05.17 2:03:21	6	2:01	11917	0	2:00	12918	0	1:58	7016	0	1:43	20176	
2012.05.17 2:04:21	7	2:03	11565	0	2:01	13267	1	1:59	6843	0	1:44	20552	
2012.05.17 2:05:21	8	2:04	11812	1	2:02	13409	1	1:59	6843	0	1:45	20875	
2012.05.17 2:06:22	9	2:05	11667	0	2:03	13130	0	1:59	6843	0	1:46	20682	
2012.05.17 2:07:22	10	2:06	12147	1	2:04	13405	1	2:00	7285	0	1:47	20446	
2012.05.17 2:08:36	10	2:06	12147	0	2:05	13222	1			0	1:47	20446	
2012.05.17 2:09:22	11	2:08	12012	1	2:06	13477	2	2:07	7357	1	1:48	21256	
2012.05.17 2:10:22	12	2:09	12070	0	2:07	13051	3	2:08	7497	0	1:49	20160	OULU (2:10)
2012.05.17 2:11:22	13	2:10	11852	1	2:08	13644	4	2:09	7431	0	1:50	20425	
2012.05.17 2:12:22	14	2:11	12152	2	2:09	13649	5	2:11	7409	0	1:50	20425	
2012.05.17 2:13:37	14			3	2:10	13426	5	2:11	7409	0	1:51	20511	FTSM (2:13)
2012.05.17 2:14:22	15	2:13	12087	4	2:11	13422	6	2:12	7351	0	1:53	20486	
2012.05.17 2:15:22	16	2:14	12198	0	2:12	13332	7	2:13	7283	0	1:53	20486	
2012.05.17 2:16:22	17	2:15	12268	1	2:13	13592	0	2:15	7136	0	1:54	20811	
2012.05.17 2:17:22	18	2:16	12203	2	2:14	13539	1	2:16	7391	0	1:57	20658	
2012.05.17 2:18:37	18	2:16	12203	3	2:15	13733	0	2:16	7391	0	1:57	20658	
2012.05.17 2:19:24	0	2:18	11943	0	2:16	13231	0	2:17	7254	1	2:03	23169	
2012.05.17 2:20:24	0	2:19	11932	0	2:17	13356	0	2:18	7352	2	2:05	23992	

Figure 6 The real-time evolution of the GLE within NMDB and the corresponding GLE alert. The relevant real-time profiles of the NMs that contributed to the real-time GLE alert are presented as well as the threshold above which each NM entered the *station alert* mode. The *general alert* was issued at 02:13 UT.

to the central GLE alert server clock is not yet ideal and needs to be revisited. To clearly assess the challenges that the real-time establishment of a GLE alert faces, we can use as an example the SOPO station. This is one of the best-suited NM stations for the detection of a GLE occurrence, nonetheless, it lost the satellite link and thus sent its data only in the aftermath of the GLE event on 17 May 2012. The APTY station has a fast rate of almost 1 min and thus is a very good example of a NM station suitable for the real-time detection of GLEs. This is also evident from the comparison between Tables 1 and 2, where the onset time for APTY was set to 01:50 (see Table 1) and the first time APTY exceeded the GLE-alert threshold was at 01:56 UT.

One should note that the GLE-alert software that has been used as an open service under the NMDB collaboration performed well during the first GLE of solar cycle 24 and issued an alert at 02:13 UT. This is because the seeders of the GLE-alert algorithm did not present a continuous data flow and good time synchronization. Nevertheless, the provision of high-quality data from the NMs resulted in a real-time automated GLE alert. Therefore, if the timing of the data is adjusted, in the sense of sending the 1-min time-resolution data of every contributing station in minute intervals into the NMDB, the real-time detection of GLEs closer to their initiation will become possible and will constitute a significant space-weather asset. It is noteworthy that the relevant real-time alert was issued by GOES based on the ≥ 100 MeV protons exceeding 1 pfu (pfu = proton flux units = particles $\mathrm{sr}^{-1}\,\mathrm{cm}^{-2}\,\mathrm{s}^{-1}$), at 02:52 UT (see http://www.swpc.noaa.gov/alerts/archive/archive_16May2012.html, for details) (Kudela, 2013).

4. Discussion and Conclusion

GLE71 is the first GLE of solar cycle 24. It is the result of a medium-strength solar flare and its corresponding CME. The release time obtained from TSA represents an estimate of the latest possible release of relativistic protons from the Sun that is consistent with the determined onset time at Earth. TSA possibly attaches the recorded particles by NMs to the shock formed by the CME, assuming a simultaneous injection of the particles at all energies.

GLE71 is, in a sense, an index of the solar activity of solar cycle 24. The importance of this event lies in the fact that so far it is the only GLE of solar cycle 24, which underlines how modest, in terms of solar activity, this solar cycle has been so far.

From the above analysis it is shown that the real-time detection of the recent GLE71 event on 17 May 2012 was possible. This confirms once again that the supporting infrastructure that was implemented within NMDB has proven to be a useful asset for the monitoring and forecasting of GLEs. NMDB managed to assemble the first operational database of NM data and has expanded over the years from a European to a global effort, leading the cosmic-ray research into the 21st century.

Given the way that the GLE alert algorithm has been developed, as we introduced in Section 3.1 and discussed in detail in Section 3.2, and from the results of Table 1, one would expect that the APTY NM would enter a *station-alert* mode on 01:54 UT and the OULU NM on 01:58 UT. Therefore the *general-alert* mode would have been established at 01:58 UT. The real-time evolution of the GLE alert, though, shows that the GLE-alert signal was established at 02:13 UT (see Figure 6 and Table 2). This is because of the lag of the 1-min time-resolution data. There are many reasons why this sometimes happens. We recall that certain NMs that are very important for establishing an accurate GLE alert are operating on very distant mountains or at polar regions, so that the communication of the 1-min time-resolution data relies on satellite links, which makes the timing a still unresolved problem that deserves to be solved. Moreover, the GLE-alert software is closely attached to the availability of real-time data and thus NM stations that provide data every 5 min or more are automatically discarded, leading to delayed alerts when both the data flow and the time synchronization are not ideal. At this point it is important to stress that this is the second successful real-time GLE alert (Souvatzoglou *et al.*, 2009) that has been issued from the same algorithm in almost six years of continuous operation. Thus, the results from the real-time GLE alert software are very promising and future work should focus on the upgrade of the software so that it becomes less dependent on the availability of real-time data.

Although there is some more distance to cover to realize the fully functional GLE alert with respect to time-synchronization problems, the basis provided by NMDB, the high quality of the neutron monitor data, and the never-ending efforts of the neutron-monitor community can easily solve pending problems and perform the necessary fine-tuning.

References

Andriopoulou, M., Mavromichalaki, H., Plainaki, C., Belov, A., Eroshenko, E.: 2011, *Solar Phys.* **269**, 155.

Bazilevskaya, G.A.: 2009, *Adv. Space Res.* **43**, 530.

Belov, A.V., Eroshenko, E.A., Kryakunova, O.N., Kurt, V.G., Yanke, V.G.: 2010, *Geomagn. Aeron.* **50**, 21.

Bieber, J.W., Dröge, W., Evenson, P.A., Pyle, R., Ruffolo, D., Pinsook, U., Tooprakai, P., Rujiwarodom, M., Khumlumlert, T., Krucker, S.: 2002, *Astrophys. J.* **567**, 622.

Bombardieri, D.J., Michael, K.J., Duldig, M.L., Humble, J.E.: 2007, *Astrophys. J.* **665**, 813.

Caballero-Lopez, R.A., Moraal, H., McDonald, F.B.: 2004, *J. Geophys. Res.* **109**, A05105.

Clem, J., Dorman, L.: 2000, *Space Sci. Rev.* **93**, 335.

Dorman, L., Zuckerman, I.: 2003, *Adv. Space Res.* **31**, 925.

Dorman, L., Pustilnik, L., Sternlieb, A., Zukerman, I., Belov, A., Eroshenko, E., *et al.*: 2004, *IEEE Trans. Plasma Sci.* **32**, 1478.

Firoz, K.A., Gan, W.Q., Moon, Y.-J., Li, C.: 2012, *Astrophys. J.* **758**, 119.

Forbush, S.E.: 1946, *Phys. Rev.* **70**, 771.

Gopalswamy, N., Xie, H., Usoskin, I.: 2010, *Indian J. Radio Space Phys.* **39**, 240.

Gopalswamy, N., Xie, H., Yashiro, S., Akiyama, S., Mäkelä, P., Usoskin, I.: 2012, *Space Sci. Rev.* **171**, 23.

Grechnev, V.V., Kurt, V.G., Chertok, I.M., Uralov, A.M., Nakajima, H., Altyntsev, A.T., *et al.*: 2008, *Solar Phys.* **252**, 149.

Kahler, S.W., Hildner, E., Van Hollebeke, M.A.I.: 1978, *Solar Phys.* **57**, 429.

Kaiser, M.L., Kucera, T.A., Davila, J.M., St. Cyr, O.C., Guhathakurta, M., Christian, E.: 2008, *Space Sci. Rev.* **136**, 5.

Kudela, K.: 2009, *Acta Phys. Slovaca* **59**, 537.

Kudela, K.: 2013, *J. Phys. Conf. Ser.* **409**, 012017.

Kurt, V., Kudela, K., Yushkov, B., Galkin, V.: 2013, *Adv. Astron.* **2013**, 690921.

Kuwabara, T., Bieber, J., Clem, J., Evenson, P., Pyle, R.: 2006, *Space Weather* **4**, S10001.

Lin, R.P., Dennis, B.R., Hurford, G.J., Smith, D.M., Zehnder, A., Harvey, P.R., *et al.*: 2002, *Solar Phys.* **210**, 3.

Malandraki, O.E., Agueda, N., Papaioannou, A., Klein, K.-L., Valtonen, E., Heber, B., *et al.*: 2012, *Solar Phys.* **579**, 233.

Mavromichalaki, H.: 2010, *Eos* **91**, 305.

Mavromichalaki, H., Souvatzoglou, G.: 2012, Online report at http://www.nmdb.eu/?q=node/480.

Mavromichalaki, H., Yanke, V., Dorman, L., Iucci, N., Chillingarian, A., Kryakunova, O.: 2004, In: Daglis, I.A. (ed.) *Effects of Space Weather on Technology Infrastructure*, *NATO Science Series II* **176**, Kluwer Academic, Dordrecht, 301.

Mavromichalaki, H., Papaioannou, A., Sarlanis, C., Souvatzoglou, G., Gerontidou, M., Plainaki, C., the NMDB Team: 2010a, In: Tsiganos, K., Hatzidimitriou, D., Matsakos, T. (eds.) *Proceedings of the 9th International Conference of the Hellenic Astronomical Society*, *ASP Conf. Ser.* **424**, 75.

Mavromichalaki, H., Souvatzoglou, G., Sarlanis, C., Mariatos, G., Papaioannou, A., Belov, A., Eroshenko, E., Yanke, V.: 2010b, *New Astron.* **15**, 744.

Mavromichalaki, H., Papaioannou, A., Plainaki, C., Sarlanis, C., Souvatzoglou, G., Gerontidou, M., the NMDB group: 2011, *Adv. Space Res.* **47**, 2210.

McComas, D.J., Bame, S.J., Barker, P., Feldman, W.C., Phillips, J.L., Riley, P., Griffe, J.W.: 1998, *Space Sci. Rev.* **86**, 563.

McCracken, K.G., Moraal, H., Shea, M.A.: 2012, *Astrophys. J.* **761**, 101.

Miroshnichenko, L., Perez-Peraza, J.: 2008, *Int. J. Mod. Phys. A* **23**, 1.

Moraal, H., McCracken, K.G.: 2012, *Space Sci. Rev.* **171**, 85.

Nitta, N.V., Liu, Y., DeRosa, M.L., Nightingale, R.W.: 2012, *Space Sci. Rev.* **171**, 61.

Papaioannou, A., Mavromichalaki, H., Gerontidou, M., Souvatzoglou, G., Nieminen, P., Glover, A.: 2011, *Astrophys. Space Sci. Trans.* **7**, 1.

Reames, D.V.: 2009, *Astrophys. J.* **693**, 812.

Robbrecht, E., Berghmans, D.: 2004, *Astron. Astrophys.* **425**, 1097.

Shea, M.A., Smart, D.F., Flückiger, E.O.: 2000, *Space Sci. Rev.* **93**, 305.

Shea, M.A., Smart, D.F.: 2012, *Space Sci. Rev.* **171**, 161.

Souvatzoglou, G., Mavromichalaki, H., Sarlanis, C., Mariatos, G., Belov, A., Eroshenko, E., Yanke, V.: 2009, *Adv. Space Res.* **43**, 728.

Steigies, C., NMDB team: 2008a, *Geophys. Res. Abstr.* **10**, EGU2008-A-00000.

Steigies, C., Thomann, M., Rother, O., Wimmer-Schweingruber, R., Heber, B.: 2008b, In: *Proc. 30th Int. Cosmic Ray Conf.* **1**, 303.

Vainio, R., Desorgher, L., Heynderickx, D., Storini, M., Flückiger, E., Horne, R.B., *et al.*: 2009, *Space Sci. Rev.* **147**, 187.

Vainio, R., Valtonen, E., Heber, B., Malandraki, O.E., Papaioannou, A., Klein, K.L., *et al.*: 2013, *J. Space Weather Space Clim.* **3**, A12.

Vashenyuk, E.V., Balabin, Yu.V., Gvozdevsky, B.B.: 2009, In: Király, P., Kudela, K., Stehlík, M., Wolfendale, A.W. (eds.) *Proc. 21st Eur. Cosmic Ray Symp.*, Institute of Experimental Physics, Slovak Academy of Sciences, Košice, Slovakia, 264.

Watanabe, K., Gros, M., Stoker, P.H., Kudela, K., Lopate, C., Valdes-Galicia, J.-F., *et al.*: 2006, *Astrophys. J.* **636**, 1135.